Appl. Phys. B 74, 489–493 (2002)
DOI: 10.1007/s003400200840

Applied Physics B
Lasers and Optics

R. DELHUILLE
C. CHAMPENOIS*
M. BÜCHNER
L. JOZEFOWSKI
C. RIZZO
G. TRÉNEC
J. VIGUÉ✉

High-contrast Mach–Zehnder lithium-atom interferometer in the Bragg regime

Laboratoire Collisions Agrégats Réactivité – IRSAMC, Université Paul Sabatier and CNRS UMR 5589, 118, Route de Narbonne, 31062 Toulouse Cedex, France

Received: 22 November 2001 /
Revised version: 10 February 2002
Published online: 24 April 2002 •

ABSTRACT We have constructed an atom interferometer of the Mach–Zehnder type, operating with a supersonic beam of lithium. Atom diffraction uses Bragg diffraction on laser standing waves. With first-order diffraction, our apparatus has given a large signal and a very good fringe contrast (74%), which we believe to be the highest ever observed with thermal atom interferometers. This apparatus will be applied to high-sensitivity measurements.

PACS 03.75.Dg; 32.80.Lg; 39.20.+q

Several different atom interferometers gave their first signals in 1991:

- a Young's double-slit experiment was demonstrated by Carnal and Mlynek, with a supersonic beam of metastable helium [1],
- a Mach–Zehnder interferometer was built by Pritchard and coworkers using a thermal atomic beam of sodium and diffraction on material gratings [2],
- an interferometer based on Ramsey fringes in saturated absorption spectroscopy, following the idea of Bordé [3], was built by Helmcke and coworkers with a thermal atomic beam of calcium, and it was used to demonstrate the Sagnac effect with atomic waves [4],
- an interferometer using a laser-cooled sodium atom and Raman diffraction was built by Kasevich and Chu, and gave the first high-sensitivity measurement of the local acceleration of gravity based on atom interferometry [5].

This research field has developed rapidly since 1991 and an excellent overview of this field and of its applications can be found in the book "Atom Interferometry" [6].

In this paper, we describe the first interference signals observed with our newly built Mach–Zehnder atom interferometer operating with thermal lithium atoms. The diffraction gratings, which are used as mirrors and beam splitters, are made of laser standing waves operating in the Bragg regime. Our first signals present a very good signal to noise ratio, a mean detected atom flux of $1.4 \times 10^4\ \mathrm{s}^{-1}$ and a 74% fringe contrast. As far as we know, this is the highest contrast ever observed with a thermal atom Mach–Zehnder interferometer.

Let us recall the performances achieved by this family of atom interferometers. In each case, we give the mean value of the detected atom flux I and the fringe contrast (or visibility) $\mathcal{C}$. These parameters are both important for phase measurements: assuming Poisson statistics for the noise, the accuracy of these measurements increases with a figure of merit given by $I\mathcal{C}^2$. In 1991, the interferometer of Pritchard and coworkers [2] gave a 13% contrast with a mean detected atom flux of $290\ \mathrm{s}^{-1}$, values improved in 1997 up to a 49% contrast and a mean flux of $1900\ \mathrm{s}^{-1}$ [7] or a 17% contrast and a mean flux of $2 \times 10^5\ \mathrm{s}^{-1}$ [8]. In 1995, Zeilinger and coworkers [9] operated an interferometer using metastable argon and laser diffraction in the Raman–Nath regime, which produced a 10% contrast associated with a mean detected flux of $1.4 \times 10^4\ \mathrm{s}^{-1}$. Also in 1995, Lee and coworkers [10] built an interferometer using metastable neon and laser diffraction in the Bragg regime and they observed a 62% contrast associated with a mean detected flux of $1.5 \times 10^3\ \mathrm{s}^{-1}$. Finally, in 2001, a helium interferometer built by Toennies and coworkers [11], with material gratings, has given a 71% contrast with a mean detected flux close to $10^3\ \mathrm{s}^{-1}$.

We have limited the present comparison to the family of interferometers which rely on elastic diffraction, i.e. in which the atom internal state is not modified by the diffraction process. However, as discussed by Bordé [3, 12], the general case is inelastic diffraction, which is used in Ramsey–Bordé interferometers [4] and also in Mach–Zehnder atom interferometers. This type of interferometer can provide a very high output flux because the various outputs are distinguished by the atom internal state and not only by the direction of propagation: this circumstance permits to use a broad (but well-collimated) atomic beam. One of the best examples is the cesium interferometer developed by Kasevich and coworkers as a gyroscope of extremely high sensitivity. This interferometer uses a thermal atomic beam of cesium, with transverse laser cooling, and it has produced a fringe contrast of 20% [13], an output flux equal to $1 \times 10^{11}\ \mathrm{s}^{-1}$ and a signal to noise ratio of 33 000 for 1 s of integration [14]. However, this advan-

✉ Fax: +33-5/6155-8317, E-mail: jacques.vigue@irsamc.ups-tlse.fr
*_Present address:_ Physique des Interactions Ioniques et Moléculaires, Université de Provence et CNRS, UMR 6633, 13397 Marseille Cedex 20, France

tage of Raman interferometers is obtained only if one does not separate the atomic paths in order to apply a perturbation to one of the two paths. This limitation is one of the reasons which explain why we have not chosen to develop a Raman interferometer.

When building an atom interferometer, two very important choices must be made, namely the atom and the diffraction process. The choice of the atom is largely limited by the possibility of producing either a very intense atomic beam or by the availability of a very high detection sensitivity. For thermal atoms, an efficient laser-induced fluorescence detection is feasible [13, 14] but difficult because the time spent in the laser-excitation volume is small. Another detection technique is based on surface ionization, which is very efficient only with alkali atoms or with metastable atoms. We have chosen to work with an alkali atom in its ground state, because the interactions of these atoms are more accurately described by ab initio quantum-chemistry calculations than those of metastable rare-gas atoms. Then, a very important design parameter is the first-order diffraction angle $\theta_1 = \lambda_{dB}/a = h/(mva)$ (where λ_{dB} is the de Broglie wavelength, a the grating period, m the atomic mass and v the velocity), as it defines the needed collimation of the atomic beam and also the separation of the atomic paths near the second grating. For supersonic beams of light alkalis seeded in a carrier gas, the beam velocity v depends almost solely on the carrier-gas molecular mass and a small velocity requires a heavy carrier gas. A convenient and inexpensive choice is argon, which gives v close to 1050 m/s for a temperature T near 1050 K.

We may compare our choices to those of Pritchard, as our interferometer design is largely inspired by his design. The choices made by Pritchard were to use material gratings with a very small a value, $a = 200$ nm in most experiments (but some experiments involved smaller values down to 100 nm) and a sodium atom (molar mass 23 g), with a de Broglie wavelength $\lambda_{dB} \approx 17$ pm and a first-order diffraction angle $\theta_1 \approx 85$ μrad. As further discussed below, we have made the choice of using laser diffraction and, in this case, the grating period is $a = \lambda_r/2$, where λ_r is the wavelength of the resonance transition. Usually, the first resonance transition is chosen for intensity reasons and practical considerations (laser cost, power and availability) and the achieved grating periods are not very small, in the 300–500-nm range. For lithium, the a value ($a = 335$ nm corresponding to $\lambda_r = 671$ nm), substantially larger than the a value commonly used by Pritchard, is compensated by the smaller mass (molar mass 7 g). With a de Broglie wavelength $\lambda_{dB} \approx 54$ pm, the first-order diffraction angle is $\theta_1 \approx 160$ μrad (from now on, we will discuss only the case of ^{7}Li, which represents 92.6% of natural lithium and which is selected by our choice of laser frequency). We want to take advantage of this relatively large diffraction angle to make interferometric experiments, with only one atomic path submitted to a perturbation. Such experiments have been done only by the group of Pritchard [15, 16], using a separation between the two atomic paths of the order of 55 μm near the second grating, while in our apparatus the corresponding separation is equal to 100 μm. Obviously, considerably larger separation values can be achieved by using a slow atomic beam, as produced by laser cooling, but, up to now, in cold-atom interferometers, the various atomic paths have not been separated because of the size of the cold samples.

Laser diffraction of atoms results from the proposal of electron diffraction by light due to Kapitza and Dirac [17], generalized to atom diffraction by Altshuler et al. [18]. In the Bragg geometry, the oscillating character of the electron-diffraction amplitude appears in the work of Federov [19] and Gush and Gush [20]. Early general theoretical analyses of laser diffraction of atoms are due to Bernhardt and Shore [21] as well as to Tanguy et al. [22]. The Rabi-oscillation regime in the Bragg geometry was discussed by Pritchard and Gould in 1985 [23] and observed by the same research group in 1987 [24]. The interest of Bragg diffraction for interferometry is that the incident beam is split almost perfectly into only two beams [12, 25] and the relative intensities of these two beams can be tuned at will by varying the laser power density and/or the interaction time. From a perturbation viewpoint, diffraction efficiency depends only on the product of these two parameters but, obviously, they are not equivalent [26, 27]. Ideally, Bragg diffraction can provide the 50% beam splitters and 100% reflective mirrors needed to build a perfect Mach–Zehnder interferometer, with a 100% transmission. On the contrary, material gratings have a low diffraction efficiency in the non-zero orders and the transmission of this type of interferometer cannot exceed a few per cent [28]. Moreover, in the case of the $^2S_{1/2} - {}^2P_{3/2}$ transition of lithium, the hyperfine structure of the excited state is very small. Then, provided that the laser detuning is large with respect to this structure and that the laser beam is linearly polarized, the potential seen by ground-state atoms is independent of the magnetic quantum number M_F but still depends on the F value because of the difference in detuning. In this case, the diffraction amplitude is the same for all the sublevels of one hyperfine level. For the experiments described below, the laser frequency is detuned on the blue side of the $^2S_{1/2} - {}^2P_{3/2}$ transition, the detuning being about 2.1 and 2.9 GHz for the $F = 1$ and $F = 2$ hyperfine states, respectively. With such a detuning, real excitation of an atom, while crossing a standing wave, has a low probability, of the order of a few per cent, so that atomic diffraction is almost perfectly coherent.

A schematic drawing of our interferometer appears in Fig. 1. An atomic beam of lithium, strongly collimated by a two-slit system, crosses three laser standing waves, which

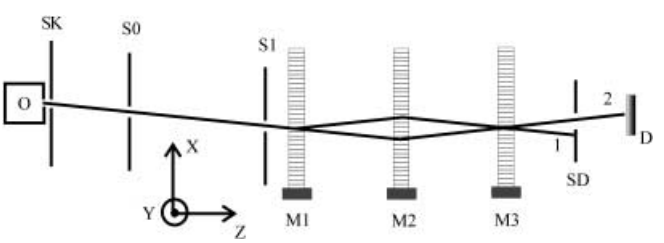

FIGURE 1 Schematic drawing of a top view of our interferometer. The x, y, z axes are represented and, for each element, we give its distance z to the nozzle. O: lithium oven; Sk: 1-mm-diameter skimmer at $z_s = 15$ mm; S_0: collimating slit of width $w_0 = 20$ μm at $z_{S_0} = 480$ mm; S_1: collimating slit of width $w_1 = 12$ μm at $z_{S_1} = 1260$ mm; M_i, $i = 1$ –3: mirrors for the laser standing waves at $z_{M_1} = 1410$ mm, $z_{M_2} = 2015$ mm and $z_{M_3} = 2620$ mm; 1 and 2: complementary exit beams; S_D: detector slit with tunable width and x position at $z_{S_D} = 3020$ mm; D: 760-μm-wide rhenium ribbon of the Langmuir–Taylor hot-wire detector at $z_D = 3370$ mm

play the role of beam splitters (first and third standing waves) and of mirrors (second standing wave). Diffraction of an atomic wave of vector $\boldsymbol{k}$ by grating G_j of wave vector $\boldsymbol{k}_{G_j}$ produces a new wave of wave vector $\boldsymbol{k}+p\boldsymbol{k}_{G_j}$, where p is the diffraction order. The two waves, exiting from the interferometer by the exit labeled 1 in Fig. 1, have the wave vectors $(\boldsymbol{k}+\boldsymbol{k}_{G_1}-\boldsymbol{k}_{G_2})$ (upper path) and $(\boldsymbol{k}+\boldsymbol{k}_{G_2}-\boldsymbol{k}_{G_3})$ (lower path). If these two wave vectors were not equal, interference fringes would appear on the detector surface and integration over the detector area would wash out the expected interference signal. Therefore, we must cancel the quantity $\Delta\boldsymbol{k}=\boldsymbol{k}_{G_1}+\boldsymbol{k}_{G_3}-2\boldsymbol{k}_{G_2}$ to optimize the fringe contrast. For a perfect interferometer [29], the two beams labeled 1 and 2 carry complementary interference signals proportional to the quantities:

$$I_{1/2}=\left[1\pm\cos\left(2\pi\left(x_{\mathrm{M}_1}+x_{\mathrm{M}_3}-2x_{\mathrm{M}_2}\right)/a\right)\right], \qquad (1)$$

where x_{M_i} is the x coordinate of mirror M_i producing the laser stationary wave and a is the corresponding grating period, $a=\lambda_{\mathrm{r}}/2=335$ nm. Therefore, interference fringes can be observed by displacing any one of the three mirrors in the x direction.

In our experiment, a supersonic beam of lithium seeded in argon (typical pressure 300 mbar) is emitted by an oven: the temperature of the oven body fixes the lithium pressure to 1.6 mbar at 1023 K (or 0.65 mbar at 973 K for some experiments), while the front part holding the 200-μm nozzle is overheated (+50 K) to prevent clogging. To insure the best stability, these temperatures are stabilized within ±1 K. The beam goes through a skimmer and enters a second vacuum chamber, where it reaches a collision-free zone. A third vacuum chamber holds the two-slit system used to strongly collimate the beam. In the fourth vacuum chamber, the atomic beam crosses three laser standing waves, each being produced by reflecting a laser beam on a mirror M_i, $i=1$–3, the distance between consecutive standing waves being 605 mm. One of the emerging atomic beams is then selected by a detector slit S_{D} whose width w_{D} and x position can be finely tuned under vacuum. Finally, this selected beam enters a UHV chamber through a 3-mm-diameter hole. This hole and the skimmer are the only collimating elements in the vertical y direction. The atoms are detected by a Langmuir–Taylor hot-wire detector using a rhenium ribbon and a channeltron. The UHV chamber is pumped by a 100-l/s turbomolecular pump (base pressure 10^{-8} mbar). The oven chamber is pumped by an unbaffled 8000-l/s oil diffusion pump, while all the other chambers are pumped by oil diffusion pumps, with water-cooled baffles, providing a base pressure near 10^{-7} mbar. Our Langmuir–Taylor hot-wire detector [30] has a detection probability for lithium atoms in the 10%–70% range, depending on rhenium surface oxidation and temperature, and a background count rate of the order of a few thousand counts/s.

The alignment of the collimating elements is simplified thanks to a laser alignment done before operation. The three mirrors M_i must be oriented within about 20 μrad, in two directions, and the final adjustments are made under vacuum by piezo mounts. The properties of a standing wave depend linearly on the orientation angles of the mirror used to reflect the laser beam, but are considerably less sensitive to the direction of this beam, which must be perpendicular to the mirror within 1 mrad only. We use 13-mm-diameter laser beams, produced by splitting the beam of an argon ion pumped cw single-frequency dye laser, after expansion by a 5× telescope.

Figure 2 shows the profile of the lithium beam diffracted by the laser standing wave corresponding to mirror M_2. This profile is recorded by moving the detector slit S_{D} (slit width $w_{\mathrm{D}}=50$ μm). After fine tuning of the angle θ_y corresponding to the rotation of this mirror around the y axis, we observe two well-resolved peaks, corresponding to the diffraction orders zero and one. The zero-order peak contains the undiffracted part of the ^{7}Li $F=1$ and 2 levels and also the ^{6}Li content of the beam for which the laser has little effect. Bragg diffraction is a Rabi-type oscillation between the two diffraction orders and the amplitude and the phase of this oscillation depend of the atom incidence angle and velocity, so that the observed diffraction efficiency results from an average over the initial conditions. From the geometry of the experiment, we have verified that the distance between the two peaks is in excellent agreement with the calculated diffraction angle. The observation of diffraction by each of the three laser standing waves serves to optimize the θ_y angle of each of the three mirrors to fulfill the Bragg condition.

We can then search for interference signals, by running simultaneously the three standing waves with incident laser powers equal to 40, 80 and 40 mW respectively, corresponding to an ideal Mach–Zehnder design. Using an autocollimator, we set the orientation angles θ_z of the three mirrors so that the vector normal to each mirror is horizontal within 50 μrad. As explained above, we must cancel the quantity $\Delta\boldsymbol{k}=\boldsymbol{k}_{G_1}+\boldsymbol{k}_{G_3}-2\boldsymbol{k}_{G_2}$, and this is done by acting on one of the three mirrors, in order to optimize the fringe contrast.

In several previous types of apparatus [2, 7, 10], the vibrational noise on the grating x positions induced a large phase noise in the interferometer, so that it was necessary to

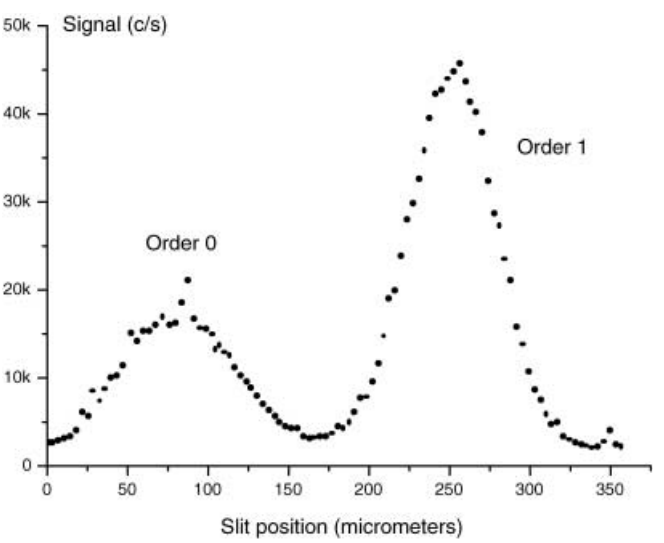

FIGURE 2 Laser diffraction of the lithium beam: number of atoms detected per second as a function of the x position (in μm) of the detector slit S_{D} (counting period: 1 s). Two peaks are observed, corresponding to the diffraction orders 0 and +1. In this experiment, only one laser standing wave, associated with mirror M_2, is present. We have verified the absence of a peak corresponding to the order −1, in agreement with the theoretical prediction for the Bragg regime. A few noise bursts of the Langmuir–Taylor hot-wire detector are visible

measure and reduce this vibrational noise before any observation. A three-grating Mach–Zehnder optical interferometer linked to the gratings can be used for this purpose [2, 10], as first done for a neutron interferometer by Gruber et al. [31]. We have also built a similar optical interferometer. Its output signal is given by (1), a being now the optical grating period ($a = 5\,\mu$m in our experiment). In our interferometer, the detected part ($x_{M_1} + x_{M_3} - 2x_{M_2}$) of the vibration-induced motion of the three mirrors has a rms value equal to 3 nm in a 50-kHz bandwidth. This very small vibrational noise is due to our construction (the interferometer mirrors are on a very rigid bench inside the vacuum chambers, which are placed on a massive support located in the basement). As the resulting phase noise, 6×10^{-2} rad, induces a negligible contrast loss, we have not tried to reduce this noise by a feedback loop.

The detector slit S_D, with a width $w_D = 30\,\mu$m, has been put at exit 1 or at exit 2 (see Fig. 1) with similar results. A slightly better fringe contrast is obtained at exit 2 than at exit 1, probably because of different contributions of stray atomic beams in the two cases. The main stray beams, which are not represented in Fig. 1, correspond to the neglected diffraction orders: they should vanish exactly if the laser power densities and the interaction times were perfectly tuned and if there was no angular and velocity dispersion of the incident atomic beam. Figure 3 presents an example of an experimental signal collected at exit 2 with a counting period equal to 0.1 s. If we subtract the background which has an average value of 3370 counts/s, we estimate the fringe contrast by:

$$\mathcal{C} = (I_{max} - I_{min})/(I_{max} + I_{min}) \approx 0.74\,.$$

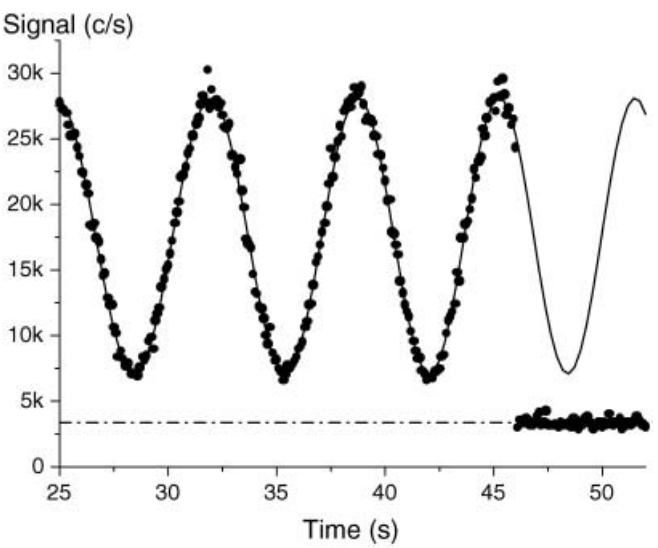

FIGURE 3 Interference fringes: number of atoms detected per second as a function of time (counting period: 0.1 s). The position x_{M_3} of mirror M_3 is swept as a function of time. We have verified that the fringe period corresponds to a displacement $\Delta x_{M_3} = \lambda_r/2 = 335$ nm. The background signal of the detector, measured by flagging the lithium beam 50 s later, is shown in the *right-hand part* of the figure and its average value 3370 counts/s is represented by the *dot-dashed line*. The data points are fitted by a sine curve, whose argument is the sum of linear and quadratic functions of time (this last term being needed to represent the piezo hysteresis). From this fit, we extract the value of the fringe contrast equal to 74% with an error of the order of 1%

A simulation of our interferometer (as in [29], but using the Bragg-diffraction amplitudes corresponding to an ideal interferometer) predicts a contrast near 90%, limited by the overlap of the exit beams 1 and 2 (see Fig. 1). The difference between this simulation and our experiment is partly due to stray beams and partly due to some phase dispersion in the interferometer. Assuming that the dominant effect is due to phase dispersion, with a Gaussian distribution and a rms value σ, the contrast is reduced by the factor $\exp(-\sigma^2/2)$. We thus deduce $\sigma \approx 0.63$ rad: in the language of the usual optics, the rms value of the wavefront defects is equal to $\lambda/10$, where λ is the atom wavelength (close to 54 pm).

Finally, we have measured the phase sensitivity of our experimental signal near 17 mrad/$\sqrt{\text{Hz}}$, not far from the shot-noise limit ≈ 10 mrad/$\sqrt{\text{Hz}}$ deduced from the signal and background count rates.

As a conclusion, we have built and operated a Mach–Zehnder Bragg atom interferometer with lithium and obtained first interference signals with an excellent signal to noise ratio and a high fringe contrast, equal to 74%. Our simulations indicate that the present fringe contrast can be improved and we expect to do so in the near future. The contrast we have observed is comparable to the contrast observed with most cold-atom interferometers (for instance [5, 32]). However, a contrast of nearly 100% has been achieved in a Mach–Zehnder Bragg interferometer using a Bose–Einstein condensate as the atomic source [33]. It is also interesting to compare our results with neutron interferometers. The technique to build such interferometers is now mature and recently built neutron interferometers [34, 35] exhibit a fringe contrast near 90%, while a 68% contrast was already observed in 1978 [36]. These very nice results suggest that an extremely high contrast is feasible. Unfortunately, the interactions of neutrons and atoms with matter and fields are extremely different so that the knowhow established with neutrons is not easily transferred to atom interferometers.

We expect to optimize our setup, in particular to increase the beam intensity by various means, including transverse laser cooling. It will also be possible to work separately with both lithium isotopes, a very interesting possibility for some applications. In our interferometer, the two atomic paths are separated by 100 μm near the second standing wave and this distance is substantially larger than in previous atom interferometers; even larger separations have been achieved by Toennies and coworkers [11]. With this new generation of interferometers, very sensitive measurements of weak perturbations are possible: with an interaction time τ of the order of 100 μs and a minimum detectable phase shift of the order of 0.1 mrad (which seems within reach, after some optimization, with an integration time of the order of a few hours), a perturbation as small as 6×10^{-16} eV can be detected. This extreme sensitivity will be used to measure atomic polarizability and index of refraction of gases for atomic waves, following the previous works of Pritchard's group [7, 15, 16].

ACKNOWLEDGEMENTS We are very much indebted to the technical staff of our laboratory, M. Gianesin, D. Castex, P. Paquier, T. Ravel, A. Pellicer, L. Polizzi and W. Volondat, for their help in building the interferometer and to several students, A. Miffre, Th. Lahaye, E. Lavallette, R. Saers,

B. Aymes and J. de Lataillade, for their contribution to the experiments. It is a pleasure to thank various colleagues, A. Bordenave-Montesquieu, J.F. Fels, J.P. Gauyacq, Siu Au Lee, H.J. Loesch, J.P. Toennies and J.P. Ziesel for their help and advice, and the 'Pôle Optique et Vision' (Saint Etienne) for laser machining of our collimating slits. Région Midi Pyrénées is gratefully acknowledged for financial support. We also thank CNRS/SPM for financial support and for a temporary position given to one of us (L.J.).

REFERENCES

1 O. Carnal, J. Mlynek: Phys. Rev. Lett. **66**, 2689 (1991)
2 D.W. Keith, C.R. Ekstrom, Q.A. Turchette, D.E. Pritchard: Phys. Rev. Lett. **66**, 2693 (1991)
3 Ch.J. Bordé: Phys. Lett. A **140**, 10 (1989)
4 F. Riehle, Th. Kisters, A. Witte, J. Helmcke, Ch.J. Bordé: Phys. Rev. Lett. **67**, 177 (1991)
5 M. Kasevich, S. Chu: Phys. Rev. Lett. **67**, 181 (1991)
6 P.R. Berman (Ed.): *Atom Interferometry* (Academic, New York 1997)
7 J. Schmiedmayer, M.S. Chapman, C.R. Ekstrom, T.D. Hammond, D.A. Kokorowski, A. Lenef, R.A. Rubinstein, E.T. Smith, D.E. Pritchard: in [1], p. 1
8 A. Lenef, T.D. Hammond, E.T. Smith, M.S. Chapman, R.A. Rubenstein, D.E. Pritchard: Phys. Rev. Lett. **78**, 760 (1997)
9 E.M. Rasel, M.K. Oberthaler, H. Batelaan, J. Schmiedmayer, A. Zeilinger: Phys. Rev. Lett. **75**, 2633 (1995)
10 D.M. Giltner, R.W. McGowan, Siu Au Lee: Phys. Rev. Lett. **75**, 2638 (1995)
11 J.P. Toennies: private communication (2001)
12 Ch.J. Bordé: in [4], p. 257
13 T.L. Gustavson, P. Bouyer, M.A. Kasevich: Phys. Rev. Lett. **78**, 2046 (1997)
14 T.L. Gustavson, A. Landragin, M.A. Kasevich: Class. Quantum Grav. **17**, 2385 (2000)
15 C.R. Ekstrom, J. Schmiedmayer, M.S. Chapman, T.D. Hammond, D.E. Pritchard: Phys. Rev. A **51**, 3883 (1995)
16 J. Schmiedmayer, M.S. Chapman, C.R. Ekstrom, T.D. Hammond, S. Wehinger, D.E. Pritchard: Phys. Rev. Lett. **74**, 1043 (1995)
17 P.L. Kapitza, P.A.M. Dirac: Proc. Camb. Phil. Soc. **29**, 297 (1933)
18 S. Altshuler, L.M. Frantz, R. Braunstein: Phys. Rev. Lett. **17**, 231 (1966)
19 M.V. Federov: Sov. Phys. JETP **25**, 952 (1967)
20 R. Gush, H.P. Gush: Phys. Rev. D **3**, 1712 (1971)
21 A.F. Bernhardt, B.W. Shore: Phys. Rev. A **23**, 1290 (1981)
22 C. Tanguy, S. Reynaud, C. Cohen-Tannoudji: J. Phys. B: At. Mol. Phys. **17**, 4623 (1984)
23 D.E. Pritchard, P.L. Gould: J. Opt. Soc. Am. B **2**, 1799 (1985)
24 P.J. Martin, B.G. Oldaker, A.H. Miklich, D.E. Pritchard: Phys. Rev. Lett. **60**, 515 (1988)
25 D.M. Giltner, R.W. McGowan, Siu Au Lee: Phys. Rev. A **52**, 3966 (1995)
26 C. Keller, J. Schmiedmayer, A. Zeilinger, T. Nonn, S. Dürr, G. Rempe: Appl. Phys. B **69**, 303 (1999)
27 C. Champenois, M. Büchner, R. Delhuille, R. Mathevet, C. Robilliard, C. Rizzo, J. Vigué: Eur. Phys. J. D **13**, 271 (2001)
28 C.R. Ekstrom: Ph.D. Thesis, MIT (1993) unpublished
29 C. Champenois, M. Büchner, J. Vigué: Eur. Phys. J. D **5**, 363 (1999)
30 R. Delhuille, A. Miffre, E. Lavalette, M. Büchner, C. Rizzo, G. Trénec, J. Vigué, H.J. Loesch, J.P. Gauyacq: Rev. Sci. Instrum., to appear
31 M. Gruber, K. Eder, A. Zeilinger, R. Gahler, W. Mampe: Phys. Lett. A **140**, 363 (1989)
32 A. Peters, K.Y. Chung, S. Chu: Nature **400**, 849 (1999)
33 Y. Torii, Y. Suzuki, M. Kozuma, T. Sugiura, T. Kuga, L. Deng, E.W. Hagley: Phys. Rev. A **61**, 041602(R) (2000)
34 D.M. Gilliam, M. Arif, D.L. Jacobson, A. Ioffe: Nucl. Instrum. Methods A **422**, 41 (1999)
35 G. Kroupa, G. Bruckner, O. Bolik, M. Zawisky, M. Hainbuchner, G. Badurek, R.J. Buchelt, A. Schricker, H. Rauch: Nucl. Instrum. Methods A **440**, 604 (2000); H. Rauch: private communication (2001)
36 W. Bauspiess, U. Bonse, H. Rauch: Nucl. Instrum. Methods **157**, 495 (1978)